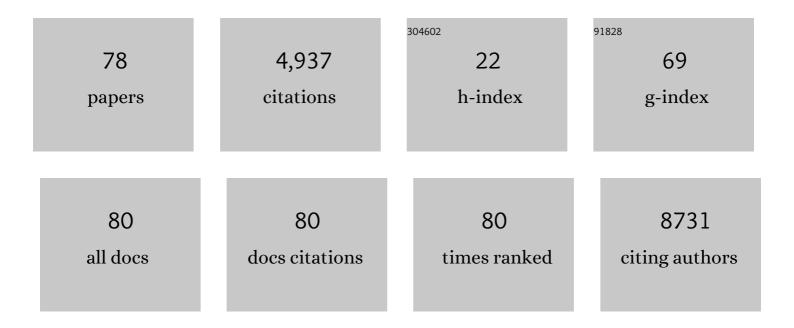
Joon Myong Song

List of Publications by Year in descending order

Source: https://exaly.com/author-pdf/7131626/publications.pdf Version: 2024-02-01



#	Article	IF	CITATIONS
1	3D bioprinted drug-resistant breast cancer spheroids for quantitative in situ evaluation of drug resistance. Acta Biomaterialia, 2022, 138, 228-239.	4.1	31
2	Scaffold-free 3D printing for fabrication of biomimetic branched multinucleated cardiac tissue construct: A promising ex vivo model for in situ detection of drug-induced sodium ion channel responses. Applied Materials Today, 2022, 27, 101416.	2.3	3
3	3D Microfluidic Platform and Tumor Vascular Mapping for Evaluating Anti-Angiogenic RNAi-Based Nanomedicine. ACS Nano, 2021, 15, 338-350.	7.3	34
4	Ag ₂ S quantum dot theragnostics. Biomaterials Science, 2021, 9, 51-69.	2.6	23
5	A 3D cell printing-fabricated HepG2 liver spheroid model for high-content <i>in situ</i> quantification of drug-induced liver toxicity. Biomaterials Science, 2021, 9, 5939-5950.	2.6	24
6	Inkjet Bioprinting on Parchment Paper for Hit Identification from Small Molecule Libraries. ACS Omega, 2020, 5, 588-596.	1.6	1
7	Application of fluorescence resonance energy transfer to bioprinting. TrAC - Trends in Analytical Chemistry, 2020, 122, 115749.	5.8	9
8	Multifunctional TPP-PEG-biotin self-assembled nanoparticle drug delivery-based combination therapeutic approach for co-targeting of GRP78 and lysosome. Journal of Nanobiotechnology, 2020, 18, 102.	4.2	22
9	Printing-Based Assay and Therapy of Antioxidants. Antioxidants, 2020, 9, 1052.	2.2	2
10	Transparent tumor microenvironment: Are liposomal nanoparticles sufficient for drug delivery to hypoxic regions and clonogenic cells?. Applied Materials Today, 2020, 19, 100561.	2.3	1
11	Side-Chain-Dependent Binding of bis-Naphthalimide Self-Assembled Nanoparticles to G-Quadruplex DNA for Potential Anticancer Therapy. ACS Applied Nano Materials, 2020, 3, 1339-1353.	2.4	3
12	Biotin-conjugated PEGylated porphyrin self-assembled nanoparticles co-targeting mitochondria and lysosomes for advanced chemo-photodynamic combination therapy. Journal of Materials Chemistry B, 2019, 7, 65-79.	2.9	56
13	Direct On-Paper Inkjet Printing of Kinase-to-Kinase Phosphorylation Cascade Reactions. ACS Omega, 2019, 4, 7866-7873.	1.6	2
14	A FRET assay for the quantitation of inhibitors of exonuclease EcoRV by using parchment paper inkjet-printed with graphene oxide and FAM-labelled DNA. Mikrochimica Acta, 2019, 186, 211.	2.5	12
15	Liposomal co-delivery-based quantitative evaluation of chemosensitivity enhancement in breast cancer stem cells by knockdown of GRP78/CLU. Journal of Liposome Research, 2019, 29, 44-52.	1.5	28
16	Inkjet printing-based photo-induced electron transfer reaction on parchment paper using riboflavin as a photosensitizer. Analytica Chimica Acta, 2018, 1012, 49-59.	2.6	13
17	Essential Role of Polo-like Kinase 1 (Plk1) Oncogene in Tumor Growth and Metastasis of Tamoxifen-Resistant Breast Cancer. Molecular Cancer Therapeutics, 2018, 17, 825-837.	1.9	46
18	Paper-based inkjet bioprinting to detect fluorescence resonance energy transfer for the assessment of anti-inflammatory activity. Scientific Reports, 2018, 8, 591.	1.6	11

#	Article	IF	CITATIONS
19	Design, synthesis, and biological evaluation of novel catecholopyrimidine based PDE4 inhibitor for the treatment of atopic dermatitis. European Journal of Medicinal Chemistry, 2018, 145, 673-690.	2.6	24
20	Inkjet printing-based β-secretase fluorescence resonance energy transfer (FRET) assay for screening of potential β-secretase inhibitors of Alzheimer's disease. Analytica Chimica Acta, 2018, 1022, 89-95.	2.6	10
21	Peptide substrate-based inkjet printing high-throughput MMP-9 anticancer assay using fluorescence resonance energy transfer (FRET). Sensors and Actuators B: Chemical, 2018, 256, 1093-1099.	4.0	12
22	Synthesis of Fluorescent Au Nanocrystals–Silica Hybrid Nanocomposite (FLASH) with Enhanced Optical Features for Bioimaging and Photodynamic Activity. Langmuir, 2018, 34, 173-178.	1.6	9
23	Investigation on vascular cytotoxicity and extravascular transport of cationic polymer nanoparticles using perfusable 3D microvessel model. Acta Biomaterialia, 2018, 76, 154-163.	4.1	26
24	High-throughput chemical screening to discover new modulators of microRNA expression in living cells by using graphene-based biosensor. Scientific Reports, 2018, 8, 11413.	1.6	17
25	A Novel Catecholopyrimidine Based Small Molecule PDE4B Inhibitor Suppresses Inflammatory Cytokines in Atopic Mice. Frontiers in Pharmacology, 2018, 9, 485.	1.6	15
26	Novel ruthenium(II) triazine complex [Ru(bdpta)(tpy)]2+ co-targeting drug resistant GRP78 and subcellular organelles in cancer stem cells. European Journal of Medicinal Chemistry, 2018, 156, 747-759.	2.6	35
27	Highâ€content cell death imaging using quantum dotâ€based TIRF microscopy for the determination of anticancer activity against breast cancer stem cell. Journal of Biophotonics, 2017, 10, 118-127.	1.1	1
28	Knockdown of clusterin alters mitochondrial dynamics, facilitates necrosis in camptothecin-induced cancer stem cells. Cell Biology and Toxicology, 2017, 33, 307-321.	2.4	24
29	Impact of Environmental Pollutant Cadmium on the Establishment of a Cancer Stem Cell Population in Breast and Hepatic Cancer. ACS Omega, 2017, 2, 563-572.	1.6	17
30	Hypermulticolor Detector for Quantum-Antibody Based Concurrent Detection of Intracellular Markers for HIV Diagnosis. Methods in Molecular Biology, 2017, 1571, 221-232.	0.4	1
31	Inkjet-Printing Enzyme Inhibitory Assay Based on Determination of Ejection Volume. Analytical Chemistry, 2017, 89, 2009-2016.	3.2	20
32	Highly Efficient and Rapid Neural Differentiation of Mouse Embryonic Stem Cells Based on Retinoic Acid Encapsulated Porous Nanoparticle. ACS Applied Materials & Interfaces, 2017, 9, 34634-34640.	4.0	19
33	Quantum-dot nanoprobes and AOTF based cross talk eliminated six color imaging of biomolecules in cellular system. Analytica Chimica Acta, 2017, 985, 166-174.	2.6	2
34	Cell death mechanistic study of photodynamic therapy against breast cancer cells utilizing liposomal delivery of 5,10,15,20-tetrakis(benzo[b]thiophene) porphyrin. Journal of Photochemistry and Photobiology B: Biology, 2017, 166, 116-125.	1.7	23
35	Synthesis, Characterization, and Antibacterial Activities of High-Valence Silver Propamidine Nanoparticles. Applied Sciences (Switzerland), 2017, 7, 736.	1.3	6
36	Bifunctional Therapeutic High-Valence Silver-Pyridoxine Nanoparticles with Proliferative and Antibacterial Wound-Healing Activities. Journal of Biomedical Nanotechnology, 2016, 12, 182-196.	0.5	21

JOON MYONG SONG

#	Article	IF	CITATIONS
37	Quantitative evaluation of ABC transporter-mediated drug resistance based on the determination of the anticancer activity of camptothecin against breast cancer stem cells using TIRF. Integrative Biology (United Kingdom), 2016, 8, 704-711.	0.6	7
38	Quantum dot as probe for disease diagnosis and monitoring. Biotechnology Journal, 2016, 11, 31-42.	1.8	52
39	Insulin-mimetic and anti-inflammatory potential of a vanadyl-Schiff base complex for its application against diabetes. RSC Advances, 2016, 6, 57530-57539.	1.7	15
40	TIRF high-content assay development for the evaluation of drug efficacy of chemotherapeutic agents against EGFR-/HER2-positive breast cancer cell lines. Analytical and Bioanalytical Chemistry, 2016, 408, 3233-3238.	1.9	2
41	Crosstalk-eliminated quantitative determination of aflatoxin B1-induced hepatocellular cancer stem cells based on concurrent monitoring of CD133, CD44, and aldehyde dehydrogenase1. Toxicology Letters, 2016, 243, 31-39.	0.4	10
42	Investigating the versatility of multifunctional silver nanoparticles: preparation and inspection of their potential as wound treatment agents. International Nano Letters, 2016, 6, 51-63.	2.3	21
43	Shape-Dependent Skin Penetration of Silver Nanoparticles: Does It Really Matter?. Scientific Reports, 2015, 5, 16908.	1.6	137
44	The Application of Bactericidal Silver Nanoparticles in Wound Treatment. Nanomaterials and Nanotechnology, 2015, 5, 23.	1.2	72
45	Spectral overlap-free quantum dot-based determination of benzo[a]pyrene-induced cancer stem cells by concurrent monitoring of CD44, CD24 and aldehyde dehydrogenase 1. Chemical Communications, 2015, 51, 2118-2121.	2.2	12
46	Cell lysis-free quantum dot multicolor cellular imaging-based mechanism study for TNF-α-induced insulin resistance. Journal of Nanobiotechnology, 2015, 13, 4.	4.2	16
47	Nanosized silver (II) pyridoxine complex to cause greater inflammatory response and less cytotoxicity to RAW264.7 macrophage cells. Nanoscale Research Letters, 2015, 10, 140.	3.1	10
48	Quantum dot nanoprobe-based high-content monitoring of notch pathway inhibition of breast cancer stem cell by capsaicin. Molecular and Cellular Probes, 2015, 29, 376-381.	0.9	27
49	Mitochondria and DNA Targeting of 5,10,15,20-Tetrakis(7-sulfonatobenzo[<i>b</i>]thiophene) Porphyrin-Induced Photodynamic Therapy via Intrinsic and Extrinsic Apoptotic Cell Death. Journal of Medicinal Chemistry, 2015, 58, 6864-6874.	2.9	72
50	Concurrent hypermulticolor monitoring of CD31, CD34, CD45 and CD146 endothelial progenitor cell markers for acute myocardial infarction. Analytica Chimica Acta, 2015, 853, 501-507.	2.6	17
51	Cytotoxicity mechanism of non-viral carriers polyethylenimine and poly-l-lysine using real time high-content cellular assay. Polymer, 2014, 55, 5178-5188.	1.8	35
52	A multifunctional composite of an antibacterial higher-valent silver metallopharmaceutical and a potent wound healing polypeptide: a combined killing and healing approach to wound care. New Journal of Chemistry, 2014, 38, 3889-3898.	1.4	18
53	Regional average intensity-based adherent cellular imaging: application to evaluation of drug-induced cardiotoxicity. Analytical Methods, 2014, 6, 6015.	1.3	0
54	"High-content quantum dot-based subtype diagnosis and classification of breast cancer patients using hypermulticolor quantitative single cell imaging cytometry― Nano Today, 2012, 7, 231-244.	6.2	25

JOON MYONG SONG

#	Article	IF	CITATIONS
55	Real-time concurrent monitoring of apoptosis, cytosolic calcium, and mitochondria permeability transition for hypermulticolor high-content screening of drug-induced mitochondrial dysfunction-mediated hepatotoxicity. Toxicology Letters, 2012, 214, 175-181.	0.4	30
56	Highly sensitive polymerase chain reaction-free quantum dot-based quantification of forensic genomic DNA. Analytica Chimica Acta, 2012, 721, 85-91.	2.6	14
57	Simultaneous analysis of Δ9-tetrahydrocannabinol and 11-nor-9-carboxy-tetrahydrocannabinol in hair without different sample preparation and derivatization by gas chromatography–tandem mass spectrometry. Journal of Pharmaceutical and Biomedical Analysis, 2011, 55, 1096-1103.	1.4	36
58	Hair analysis and self-report of methamphetamine use by methamphetamine dependent individuals. Journal of Chromatography B: Analytical Technologies in the Biomedical and Life Sciences, 2011, 879, 541-547.	1.2	36
59	VEGF inhibitor (Iressa) arrests histone deacetylase expression: Singleâ€cell cotransfection imaging cytometry for multiâ€ŧargetâ€multiâ€drug analysis. Journal of Cellular Physiology, 2011, 226, 2115-2122.	2.0	4
60	Quantification of UV-induced cyclobutane pyrimidine dimers using an oligonucleotide chip assay. Analytical and Bioanalytical Chemistry, 2010, 397, 2271-2277.	1.9	3
61	Development of radiation indicators to distinguish between irradiated and non-irradiated herbal medicines using HPLC and GC-MS. Analytical and Bioanalytical Chemistry, 2010, 398, 943-953.	1.9	8
62	Pulsed photostimulated- and thermo-luminescence investigations of Î ³ ray-irradiated herbs. Food Chemistry, 2010, 122, 1290-1297.	4.2	11
63	High-throughput screening of xanthine oxidase inhibitory properties of drug analogs using photodiode array microchip. , 2010, , .		Ο
64	Silver as antibacterial agent: Metal nanoparticles to nanometallopharmaceuticals: (Silver based) Tj ETQq0 0 0 rg	gBT /Overlo	ock 10 Tf 50 3
65	On chip superoxide dismutase assay for high-throughput screening of radioprotective activity of herbal plants. , 2010, , .		1
66	Multicolor single cell imaging cytometry: A new drug screening platform for monitoring intracellular caspases as potential therapeutic targets. , 2010, , .		0
67	Evaluation of passive mixing behaviors in a pillar obstruction poly(dimethylsiloxane) microfluidic mixer using fluorescence microscopy. Microfluidics and Nanofluidics, 2009, 7, 267-273.	1.0	49
68	Development of a photosensitive, high-throughput chip-based superoxide dismutase (SOD) assay to explore the radioprotective activity of herbal plants. Biosensors and Bioelectronics, 2009, 24, 3587-3593.	5.3	8
69	Interdigitated microelectrode array-coupled bipolar semiconductor photodiode array (IMEA-PDA) microchip for on-chip electrochemiluminescence detection. Biomedical Microdevices, 2009, 11, 971-980.	1.4	5
70	Identification of Î ³ -ray irradiated medicinal herbs using pulsed photostimulated luminescence, thermoluminescence, and electron spin resonance spectroscopy. Analytical and Bioanalytical Chemistry, 2009, 394, 1931-1945.	1.9	6
71	Synthesis of Highly Antibacterial Nanocrystalline Trivalent Silver Polydiguanide. Journal of the American Chemical Society, 2009, 131, 16147-16155.	6.6	68
72	Photodiode Array On-chip Biosensor for the Detection of E. coli O157:H7 Pathogenic Bacteria. Methods in Molecular Biology, 2009, 503, 325-335.	0.4	10

JOON MYONG SONG

#	Article	IF	CITATIONS
73	Green fluorescent protein (GFP) as a direct biosensor for mutation detection: Elimination of false-negative errors in target gene expression. Analytical Biochemistry, 2008, 380, 91-98.	1.1	7
74	Does the Antibacterial Activity of Silver Nanoparticles Depend on the Shape of the Nanoparticle? A Study of the Gram-Negative Bacterium Escherichia coli. Applied and Environmental Microbiology, 2007, 73, 1712-1720.	1.4	3,422
75	Determination of the dose–depth distribution of proton beam using resazurin assay in vitro and diode laser-induced fluorescence detection. Analytica Chimica Acta, 2007, 593, 214-223.	2.6	15
76	Development of a novel DNA chip based on a bipolar semiconductor microchip system. Biosensors and Bioelectronics, 2007, 22, 1447-1453.	5.3	12
77	Low noise bipolar photodiode array protein chip based on on-chip bioassay for the detection of E. coli O157:H7. Biomedical Microdevices, 2007, 9, 565-572.	1.4	7
78	DNA mutation analysis based on capillary electrochromatography using colloidal poly(N-isopropylacrylamide) particles as pseudostationary phase. Talanta, 2006, 68, 940-944.	2.9	13